Journal of Magnetism and Magnetic Materials 425 (2017) 20–24

Contents lists available at ScienceDirect

Journal of Magnetism and Magnetic Materials

journal homepage: www.elsevier.com/locate/jmmm

Energy-based ferromagnetic material model with magnetic anisotropy

Simon Steentjes[a,*], François Henrotte[b], Kay Hameyer[a]

[a] Institute of Electrical Machines - RWTH Aachen University, Schinkelstr. 4, D-52056 Aachen, Germany
[b] Institute of Mechanics Materials and Civil Engineering - UCL, Av. G. Lemaître 4-6, B-1348 Louvain-la-Neuve, Belgium

ARTICLE INFO

Keywords:
Hysteresis modeling
Magnetic anisotropy
Magnetostriction
Thermodynamics

ABSTRACT

Non-oriented soft magnetic materials are commonly assumed to be magnetically isotropic. However, due to the rolling process a preferred direction exists along the rolling direction. This uniaxial magnetic anisotropy, and the related magnetostriction effect, are critical to the accurate calculation of iron losses and magnetic forces in rotating electrical machines. This paper proposes an extension of an isotropic energy-based vector hysteresis model to account for these two effects.

1. Introduction

Non-oriented soft magnetic materials are widely used as a basic constituent in rotating electrical machines. Although their qualification seems to indicate them to be magnetically isotropic, they exhibit actually, due to the rolling process, a magnetically preferred direction that leads to anisotropy in both the magnetic and elastic behavior [1]. A variety of vector hysteresis models have been developed to simulate the magnetization process under rotational field. Many of them are vector extension of well-established uniaxial scalar models; the vectorization being realized by superposition of a number of scalar models oriented over different directions [2–4]. In contrast, the model presented in this paper builds on an isotropic energy-based vector hysteresis model [5–7], which is inherently a vector model and offers readily a complete theoretical framework to include magnetic anisotropy, magnetostriction, and characteristic features of magnetic hysteresis such as the wiping-out property or rotational hysteresis.

2. Energy-based ferromagnetic material model

The proposed model builds on the thermodynamic representation of hysteresis proposed in [5–8] and gets some inspiration from the kinematic hardening theory of plasticity discussed in [9–11].

2.1. Magnetic state variables

To appropriately account for the susceptibility of empty space, the magnetic flux density $\mathbf{b}$ is represented as a sum of two components (1): an empty space magnetic polarization $\mathbf{J}_0=\mu_0\mathbf{h}$ (with μ_0 the magnetic permeability of vacuum), which is always present, and a material magnetic polarization $\mathbf{J}$, associated with the presence of microscopic moments attached to the atoms of a material body.

$$\mathbf{b} = \mathbf{J}_0 + \mathbf{J} \tag{1}$$

2.2. Energy conservation

The ferromagnetic material model follows from the expression of the conservation of energy in the material

$$\mathbf{h}\cdot\dot{\mathbf{b}} = \dot{U} + D \tag{2}$$

where U is the internal energy density, $\mathbf{h}\cdot\dot{\mathbf{b}}$ the rate of magnetic work, and $D\geq 0$ a non-negative dissipation functional. Note that the terms of the energy conservation equation have actually the dimension of power.

2.3. Internal energy and anhysteretic saturation

The internal energy U is a function of the state variables of the system and is composed of two terms. The first term depends on $\mathbf{J}_0$ and accounts for the energy of empty space. The second term $u(\mathbf{J}, \ldots)$ accounts for the energy stored in matter and depends on $\mathbf{J}$ and possibly on other nonmagnetic state variables (strain, entropy, ...). The variation in time of the internal energy, holding non-magnetic state variables constant, writes

$$\dot{U} = \frac{\mathbf{J}_0}{\mu_0}\cdot\dot{\mathbf{J}}_0 + \partial_{\mathbf{J}}u(\mathbf{J}, \ldots)\cdot\dot{\mathbf{J}}. \tag{3}$$

The second term can be regarded as the power delivered to the state

* Corresponding author.
E-mail addresses: simon.steentjes@iem.rwth-aachen.de (S. Steentjes), francois.henrotte@uclouvain.be (F. Henrotte).

http://dx.doi.org/10.1016/j.jmmm.2016.10.085
Received 31 May 2016; Received in revised form 23 September 2016; Accepted 16 October 2016
Available online 19 October 2016
0304-8853/

variable **J** by a magnetic field $\mathbf{h}_r$ called reversible magnetic field. The anhysteretic saturation curve of the material is the 1-1 relationship between the (dual) quantities $\mathbf{h}_r$ and **J**. This material characteristic and its inverse are noted

$$\mathbf{h}_r = \partial_{\mathbf{J}} u(\mathbf{J}, \ldots), \quad \mathbf{J} = \mathbf{J}_{\text{an}}(\mathbf{h}_r) \tag{4}$$

Here, $\mathbf{J}_{\text{an}}$ the anhysteretic magnetization curve, which is scalar and one-to-one. Experiments show that the anhysteretic curve can be represented accurately with a double Langevin function, although it cannot be given easily a theoretical ground with the statistical approach. In consequence, we shall not regard the double Langevin representation as a fundamental aspect of the energy based hysteresis model, but rather use it as a convenient tool to accurately represent the anhysteretic curve with a smooth easily differentiable function. Practically, in the saturable isotropic case, the vectors **J** and $\mathbf{h}_r$ are collinear and the characteristics (4) are written in terms of a scalar magnetic reluctivity $\nu(J)$ and a scalar magnetic permeability $\mu(h)$ as

$$\mathbf{h}_r = \nu(|\mathbf{J}|)\ \mathbf{J}, \quad \mathbf{J} = \mu(|\mathbf{h}_r|)\ \mathbf{h}_r \tag{5}$$

2.4. Magnetic hysteresis

Magnetic hysteresis can be brought into the model in terms of the mechanical analogy depicted in Fig. 1. The pinning force that opposes the motion of Bloch walls in the ferromagnetic material is the analogous of the dry friction force represented by the slider, and the corresponding non-negative dissipation functional writes

$$D = \kappa\ |\dot{\mathbf{J}}| = \mathbf{h}_i \cdot \dot{\mathbf{J}} \tag{6}$$

with κ in A/m a material characteristic called *pinning field* (Fig. 1). We require the dissipation D to be the power delivered by a magnetic field $\mathbf{h}_i$ called irreversible magnetic field, as the magnetic polarization **J** varies in time. There is no dissipation in empty space associated with the variation of $\mathbf{J}_0$. The algebraic expression of $\mathbf{h}_i$ is not straightforwardly derived from the definition (6). The functional $\kappa\ |\dot{\mathbf{J}}|$ is indeed not differentiable at $\dot{\mathbf{J}} = 0$, and one is therefore not allowed to simply write $\mathbf{h}_i = \partial_{\dot{\mathbf{J}}} D$. The functional is nonetheless convex, and one resorts to the concept of subgradient, a generalization of the concept of gradient valid for convex functionals. One writes

$$\mathbf{h}_i \in \partial_{\dot{\mathbf{J}}} D \tag{7}$$

where the set

$$\partial_{\dot{\mathbf{J}}} D = \{\mathbf{h}_i,\ |\mathbf{h}_i| \le \kappa \ \text{ if} \dot{\mathbf{J}} = 0,\quad \mathbf{h}_i = \kappa \frac{\dot{\mathbf{J}}}{|\dot{\mathbf{J}}|} \ \text{ if} \dot{\mathbf{J}} \neq 0\}.$$

Energy conservation can now be rewritten into the identity

$$\left(\mathbf{h} - \frac{\mathbf{J}_0}{\mu_0}\right) \cdot \dot{\mathbf{J}}_0 + (\mathbf{h} - \mathbf{h}_r - \mathbf{h}_i) \cdot \dot{\mathbf{J}} = 0, \tag{8}$$

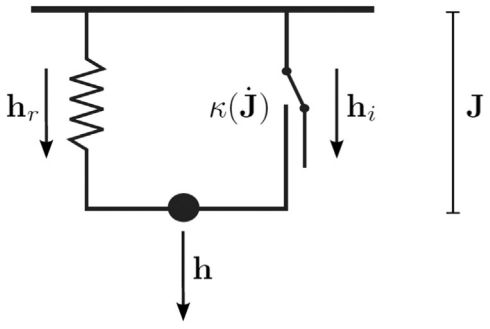

Fig. 1. Lumped parameter mechanical analogy for magnetic hysteresis as a nonlinear spring in parallel with a slider.

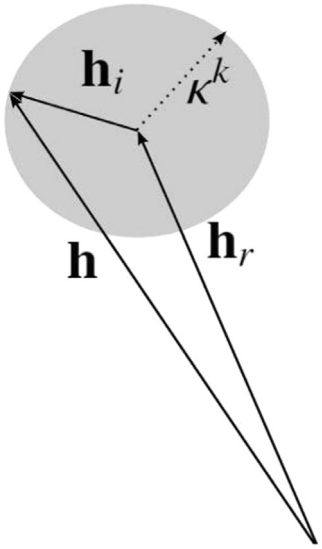

Fig. 2. Graphical representation of the vector equation $\mathbf{h}=\mathbf{h}_r+\mathbf{h}_i$ in the isotropic case.

that must hold for arbitrary $\dot{\mathbf{J}}_0$ and, hence a definition for $\mathbf{J}_0$: $\mathbf{J}_0=\mu_0\mathbf{h}$ and the nonlinear differential equation in **J** (9) to be solved at each time step.

$$\mathbf{h} - \partial_{\mathbf{J}} u(\mathbf{J}, \ldots) \in \partial_{\dot{\mathbf{J}}} D \tag{9}$$

This at first sight obscure differential equation can be given a clear pictorial representation, Fig. 2 (isotropic case) The grey sphere centred at $\mathbf{h}_r$ is the representation of the subgradient. Starting from the situation depicted in Fig. 2, if the tip of applied magnetic field **h** enters the sphere, one has $|\mathbf{h}_i| = |\mathbf{h} - \mathbf{h}_r| \le \kappa$and the reversible magnetic component $\mathbf{h}_r$ is unmodified, and hence $\dot{\mathbf{J}} = 0$, since $\mathbf{h}_r$ and **J** are in a 1-1 relationship. Both quantities remain unmodified as long as the tip of **h** remains inside the sphere. If now **h** tends to reach out of the sphere, which is forbidden by the inclusion condition in (9), the sphere must be shifted. In this case, one has , and an evolution equation for **J**:

$$\mathbf{h} = \partial_{\mathbf{J}} u(\mathbf{J}, \ldots) + \kappa \frac{\dot{\mathbf{J}}}{|\dot{\mathbf{J}}|} \tag{10}$$

In a real material, the pinning field κ cannot be represented by a single constant. An accurate hysteresis model requires considering a distribution of pinning fields, the characteristics of which vary largely across the different types of soft ferromagnetic materials [12]. We show first how to account for this distribution in the theory, leaving it for Ref. [12] to discuss how it can be identified from measurements. In order to describe hysteresis, the soft magnetic material is regarded as a set of independent abstract domains, called pinning domains, characterized each by a particular value κ^k of the pinning force (Fig. 3). Let ω^k, a partition of unity $\sum_k \omega^k=1$, be the probability that a magnetic moment in the material belongs to the domain with pinning field κ^k, of which the magnetic state is described by a magnetic polarization $\mathbf{J}^k$. One has $\mathbf{b}=\mathbf{J}_0+\sum_k \mathbf{J}^k$, and the energy density of the material, and its time derivative (holding all nonmagnetic state variables constant), write respectively

$$U = \frac{|\mathbf{J}_0|^2}{2\mu_0} + \sum_k \omega^k u\left(\frac{\mathbf{J}^k}{\omega^k}, \ldots\right), \quad \dot{U} = \frac{\mathbf{J}_0}{\mu_0} \cdot \dot{\mathbf{J}}_0 + \sum_k \mathbf{h}_r\left(\frac{\mathbf{J}^k}{\omega^k}, \ldots\right) \cdot \dot{\mathbf{J}}^k \tag{11}$$

in terms of the state variables $\mathbf{J}^k$. The dissipation functional, on the other hand, is the algebraic sum of the dissipation in the different domains

$$D = \sum_k \kappa^k |\dot{\mathbf{J}}^k| = \sum_k \mathbf{h}_i^k \cdot \dot{\mathbf{J}}^k \quad \text{with} \quad \mathbf{h}_i^k \in \partial_{\dot{\mathbf{J}}^k} D \tag{12}$$

and

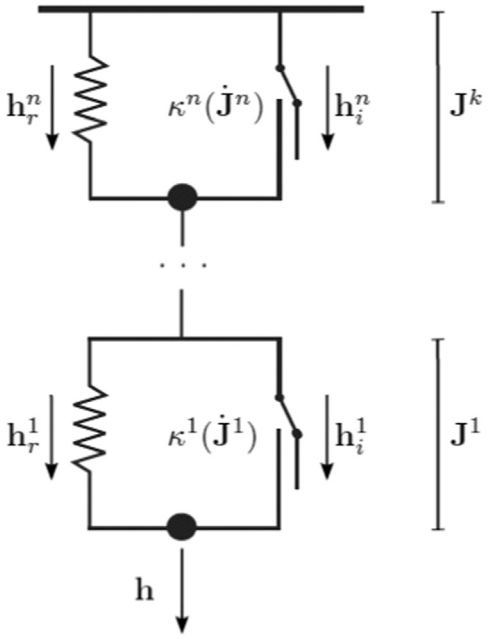

Fig. 3. Pictorial representation of the model with N internal variables.

$$\partial_{\mathbf{J}^k} D = \{\mathbf{h}_i^k,\ |\mathbf{h}_i^k| \le \kappa^k \ \text{if} \dot{\mathbf{J}}^k = 0,\quad \mathbf{h}_i^k = \kappa^k \frac{\dot{\mathbf{J}}^k}{|\dot{\mathbf{J}}^k|} \ \text{if} \dot{\mathbf{J}}^k \neq 0\} \tag{13}$$

These terms can now be summed up to obtain the relationship

$$\left(\mathbf{h} - \frac{\mathrm{J}_0}{\mu_0}\right)\cdot\dot{\mathbf{J}}_0 + \left(\mathbf{h} - \mathbf{h}_r\left(\frac{\mathbf{J}^k}{\omega^k}\right) - \mathbf{h}_i^k(\mathbf{J}^k)\right)\cdot\dot{\mathbf{J}}^k = 0, \tag{14}$$

which must hold for arbitrary $\dot{\mathbf{J}}^k$, hence the nonlinear differential equation in $\mathbf{J}^k$

$$\mathbf{h} - \mathbf{h}_r\left(\frac{\mathbf{J}^k}{\omega^k}\right) \in \partial_{\mathbf{J}^k} D \tag{15}$$

to be solved at each time step in each domain.

3. Magnetic anisotropy

Soft magnetic steel laminations produced by a rolling process have a crystallographic texture in which the crystals have a preferred orientation. Such materials exhibit at the macroscopic scale a uni-axial kind of anisotropy for which the rolling direction (RD) must be distinguished for the transverse directions (TD) [13]. We want to adapt the material model for such materials and seek for an implementation consistent from the point of view of both geometry and energy conservation.Macroscopic anisotropy has an effect on both the coercive field and the anhysteretic curve. The latter can be accounted for by replacing the scalar magnetic reluctivity $\nu(J)$ with a tensorial magnetic reluctivity $\nu(J)\boldsymbol{G}(\gamma)$ where the tensor (the undotted product of vectors **ab** is the dyadic product)

$$\boldsymbol{G}(\gamma) = \mathbf{e}_{\|}\mathbf{e}_{\|} + \gamma^2 \mathbf{e}_{\perp}\mathbf{e}_{\perp} \tag{16}$$

is defined as a function of a scalar parameter γ, $\gamma > 1$, and the microstructure-anchored unit vectors $\mathbf{e}_{||}$ and $\mathbf{e}_{\perp}$ in rolling and transverse direction respectively (they are unitary in the reference configuration). Hence, the anisotropic version of the saturation law (4), (5) writes

$$\mathbf{h}_r = \nu(|\mathbf{J}|)\ \boldsymbol{G}(\gamma)\,\mathbf{J} \tag{17}$$

$$\mathbf{J} = \mathbf{J}_{\mathrm{an}}(\boldsymbol{G}^{-1}(\gamma)\,\mathbf{h}_r) = \mu(\ |\boldsymbol{G}^{-1}(\gamma)\,\mathbf{h}_r|\ )\ \boldsymbol{G}^{-1}(\gamma)\,\mathbf{h}_r \tag{18}$$

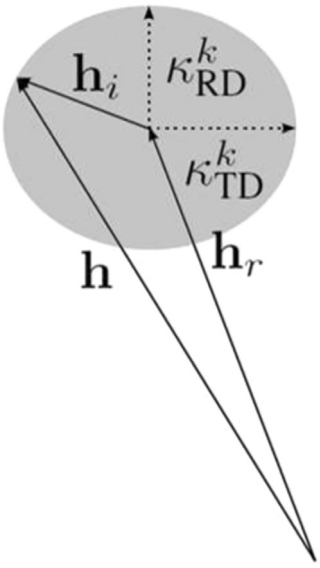

Fig. 4. Graphical representation of the vector equation $\mathbf{h}=\mathbf{h}_r+\mathbf{h}_i$ in the anisotropic case.

On the other hand, the effect of magnetic anisotropy on the coercivity of the material is represented in the hysteresis model by flattening the spheres of the isotropic model in RD, Fig. 4. The scalar pinning force κ^k does not become a tensor, however, because the magnetic field $\mathbf{h}_i$ must by definition remain collinear with the variation of the magnetic polarization $\dot{\mathbf{J}}$. Anisotropy is represented by having the pinning force κ^k be a function of the angle between $\dot{\mathbf{J}}$ and $\mathbf{e}_{||}$, e.g.,

$$\kappa^k(\alpha, \gamma') = \kappa^k_{RD}(1 + (\gamma' - 1)\,(1-\alpha^2)) \tag{19}$$

where $\alpha = \dot{\mathbf{J}}\cdot\mathbf{e}_{\|}$ is the direction cosine of $\dot{\mathbf{J}}$ in rolling direction if $\dot{\mathbf{J}} \neq 0$, else $\alpha = \mathbf{h}_i\cdot\mathbf{e}_{\|}$. The anisotropic extension of the material model (15) writes thus

$$\mathbf{h} - \nu\left(\frac{|\mathbf{J}^k|}{\omega^k}\right)\boldsymbol{G}(\gamma)\frac{\mathbf{J}^k}{\omega^k} \in \partial_{\mathbf{J}^k} D, \ \text{with} \tag{20}$$

$$\partial_{\mathbf{J}^k} D = \{\mathbf{h}_i^k,\ |\mathbf{h}_i^k| \le \kappa^k(\mathbf{h}_i\cdot\mathbf{e}_{\|},\ \gamma')\ \text{if}\ \dot{\mathbf{J}}^k = 0,\quad \mathbf{h}_i^k = \kappa^k(\dot{\mathbf{J}}\cdot\mathbf{e}_{\|},\ \gamma')\,\frac{\dot{\mathbf{J}}^k}{|\dot{\mathbf{J}}^k|}\ \text{if}\ \dot{\mathbf{J}}^k \neq 0\}.$$

It is sufficient for the anisotropic extension of the material model to identify the scalar parameters γ and γ'. More involved expressions of (16) and (19) with more parameters, or additional unit vectors associated with other significant directions of easy magnetization, can be used if needed, and if there is enough experimental data to identify them. As we are dealing here with the uniaxial anisotropy of standard electric steel laminations, we proceed with anisotropy represented by just these two scalar parameters. Finally, it must be noted that the governing equation of the differential model only involves the gradient and the subgradient of the energy functionals describing the material. Those gradients are the constitutive relationships of the material, and they can be identified in principle from measurements of the physical quantities **b** and **h** of the system.

The functionals u and D, on the other hand, are not directly measurable. They are obtained by an appropriate integration of the measured (sub)gradients in the state space of the material. This extra integration step might however be quite tedious in practice or even impossible analytically. A variational approach to solve the problem is therefore impossible in many cases, especially when the complexity of the material model increases, whereas the differential approach is always available.

4. Implementation

First of all, the vector quantity $\mathbf{h}_r\left(\frac{\mathbf{J}^k}{\omega^k}\right)$ must be recorded in each pinning domain to account for the memory effect. Let thus $\mathbf{h}_{rp}^k$ be the value of $\mathbf{h}_r\left(\frac{\mathbf{J}^k}{\omega^k}\right)$ at the previous time step. In order to solve (20) in the pinning domain k, it is useful to define the auxiliary quantities, $\mathbf{x}:=\boldsymbol{G}^{-1}(\gamma)\,\mathbf{h}_r\left(\frac{\mathbf{J}^k}{\omega^k}\right)$ and $\mathbf{x}_p:=\boldsymbol{G}^{-1}(\gamma)\,\mathbf{h}_{rp}^k$ in terms of which the variation of the magnetic polarization can be linearized as

$$\frac{\dot{\mathbf{J}}^k}{\omega^k}=\partial_t \mathbf{J}_{\mathrm{an}}(\mathbf{x})=\partial_t\{\mu(|\mathbf{x}|)\;\mathbf{x}\}$$
$$=\{\mu(|\mathbf{x}|)\,\boldsymbol{I}+2\,\partial_{h2}\mu(|\mathbf{x}|)\;\mathbf{x}\mathbf{x}\}\;\dot{\mathbf{x}}:=\mu^{\partial}(\mathbf{x})\;\dot{\mathbf{x}},$$

and then, at first order,

$$\frac{\dot{\mathbf{J}}^k}{|\dot{\mathbf{J}}^k|}=\frac{\mu^{\partial}(\mathbf{x})\;\dot{\mathbf{x}}}{|\mu^{\partial}(\mathbf{x})\;\dot{\mathbf{x}}|}\approx\frac{\mu^{\partial}(\mathbf{x}_p)\,(\mathbf{x}-\mathbf{x}_p)}{|\mu^{\partial}(\mathbf{x}_p)\,(\mathbf{x}-\mathbf{x}_p)|} \tag{21}$$

with $\mathbf{x}_P$ the value of $\mathbf{x}$ at the previous time step. The nonlinear differential Eq. (21) can then be solved by the following procedure. Let $\mathbf{h}$ be the value of the applied magnetic field at time t. The pinning domains are considered one after the other. If $|\mathbf{h}-\mathbf{h}_{rp}^k|\le\kappa^k((\mathbf{h}-\mathbf{h}_{rp}^k)\cdot\mathbf{e}_{\|},\gamma')$, the magnetic state of the domain is left unmodified by the new value of $\mathbf{h}$, i.e., $\dot{\mathbf{J}}^k=0$, and one has simply $\mathbf{x}=\mathbf{x}_P$. Otherwise, $\dot{\mathbf{J}}^k\neq 0$, and the updated value of $\mathbf{x}$ is obtained by solving the nonlinear implicit differential equation in $\mathbf{x}$

$$\mathbf{h}=\boldsymbol{G}(\gamma)\,\mathbf{x}+\kappa^k(\dot{\mathbf{J}}\cdot\mathbf{e}_{\|},\gamma')\,\frac{\mu^{\partial}(\mathbf{x}_p)\,(\mathbf{x}-\mathbf{x}_p)}{|\mu^{\partial}(\mathbf{x}_p)\,(\mathbf{x}-\mathbf{x}_p)|}, \tag{22}$$

which can be solved efficiently with a bracketing root finding method.

5. Application

The materials under study, referenced as M235-35A and M400-50A, are non-oriented FeSi steel lamination with 3.2% and 2.4% Si of thickness of 0.35 mm and 0.5 mm, respectively. The measurements are done under standardized Epstein frame protocols. Epstein frames are measurement apparatus utilizing the field-metric method under sinusoidal magnetic flux densities. They are equipped with different number of primary and secondary windings for different frequency ranges. Quasi-static material characteristics, on the other hand, are identified by point-by-point DC-measurements using a flux-meter. The covered magnetic flux density range is 0.1–1.5 T. The Epstein frame used in this study has 24 stripes (of dimension 280 mm × 30 mm). Model parameters are identified according to the methodologies described in [7,12]. Comparisons of the anisotropic model with measurements of the two materials are presented in Figs. 5–8. It is apparent that the anisotropy effects can be described by the two parameters, in particular the effect on the virgin curves. A disagreement between the measured and the modelled hysteresis loops indeed exists, especially around the reversal points. This is an accepted limitation of our energy-based hysteresis model, which could be raised by using a more complex cell description. This is however beyond the scope of this paper devoted to the specific representation of anisotropy effects.

6. Conclusion

The motivation for this work is the development of constitutive models for hysteresis phenomena accounting for the magnetic anisotropy in textured non-oriented electrical steel sheets. The proposed model, based on thermodynamic principles, is energy-consistent. A practical implicit update rule exists. Besides mathematical and physical elegance, this model has practical advantages. It is readily vectorial and the number of parameters is not limited. Moreover, it relies on an energy balance, of which the stored magnetic energy and dissipated energy are known at all times. With this approach, hysteresis losses, accounting for vector effects (rotating hysteresis) and the presence of higher harmonics, can be evaluated with controllable accuracy. This opens up the possibility of accurate evaluations of magnetic losses in real-life electrical engineering devices: From the prediction of iron losses in electrical engineering devices (rotating machines, actuators, brakes) to the accurate modeling of hysteresis in magnetostrictive

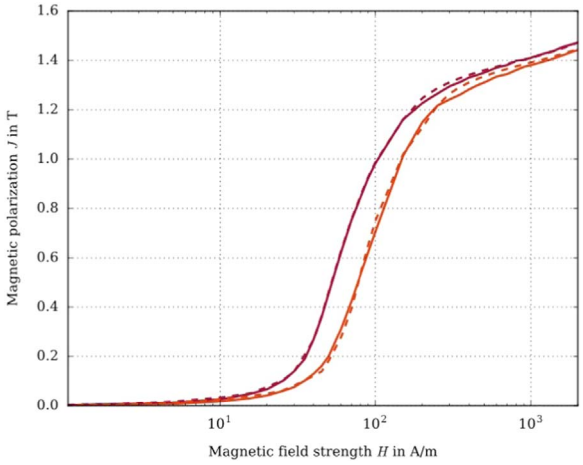

Fig. 5. Comparison of simulated (dotted lines) and measured (continuous lines) quasi-static virgin curves of M235-35A in rolling and transversal direction.

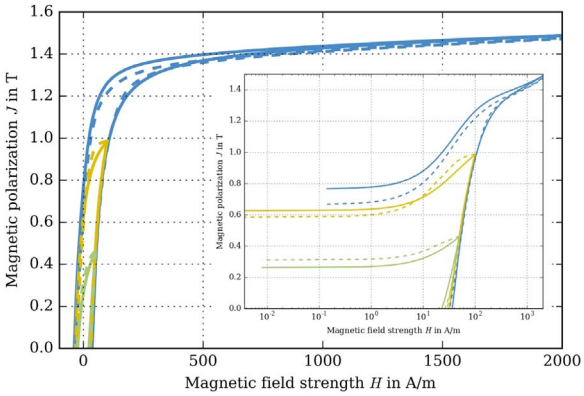

Fig. 6. Comparison of simulated (dashed lines) and measured (continuous lines) quasi-static hysteresis loops of M235-35A in rolling (0°) direction. The inset depicts the obtained loops using a logarithmic scale of the abscissa.

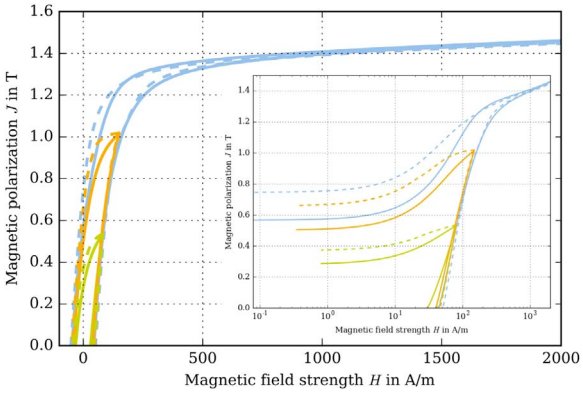

Fig. 7. Comparison of simulated (dashed lines) and measured (continuous lines) quasi-static hysteresis loops of M235-35A in transversal direction. The inset depicts the obtained loops using a logarithmic scale of the abscissa.

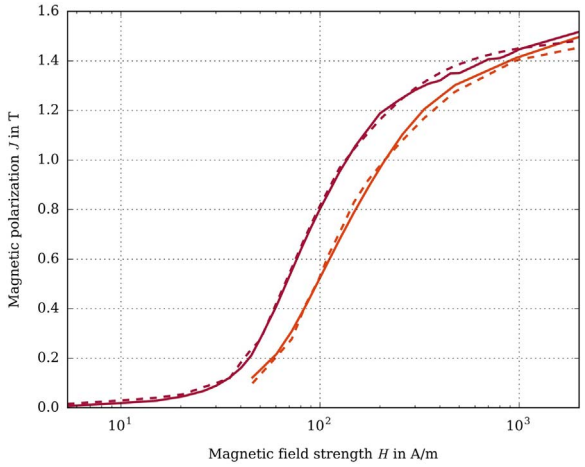

Fig. 8. Comparison of simulated (dotted lines) and measured (continuous lines) quasi-static virgin curves of M400-50A in rolling and transversal direction.

actuators and smart materials. The hysteresis model proposed in this paper represents a significant improvement with respect to conventional post-processing techniques based on measured loss characteristics. Because it relies on a physical assumption that it is vectorial from the beginning (the analogy with a dry friction force), the identified parameters represent the material in general, and not under specific experimental conditions. In other words, although the identification was done with experimental data assuming a sinusoidal in time and unidirectional **b** field, the identified parameters can be used in 2D and 3D, and in the presence of higher harmonics.

References

[1] C.W. Chen, Magnetism and Metallurgy of Soft Magnetic Materials, North-Holland Publishing Company, Amsterdam, Netherlands, 1977.
[2] I. Mayergoyz, Mathematical Models of Hysteresis and their Applications: Second Edition, Academic Press, New York, USA, 2003.
[3] G. Bertotti, Hysteresis in Magnetism, Academic Press, New York, USA, 1998, pp. 479–503.
[4] E. Cardelli, A. Faba, Numerical two-dimensional modeling of grain oriented steel, J. Appl. Phys. 115 (2014) 17A327.
[5] A. Bergqvist, Magnetic vector hysteresis model with dry friction-like pinning, Physica B 233 (1997) 342–347.
[6] F. Henrotte, K. Hameyer, A dynamical vector hysteresis model based on an energy approach, IEEE Trans. Magn. 43 (4) (2006) 899–902.
[7] S. Steentjes, F. Henrotte, C. Geuzaine, K. Hameyer, A dynamical energy-based hysteresis model for iron loss calculation in laminated cores, Int. J. Numer. Model.: Electron. Netw. Devices Fields 27 (3) (2013) 433–443.
[8] F.Henrotte, A.Nicolet, K.Hameyer, An energy-based vector hysteresis model for ferromagnetic model, in: Proceedings of the Selected Papers from the EPNC'2004 Symposium, Poznan, Poland, June 2004, pp. 28–30.
[9] A.M. Puzrin, G.T. Houlsby, Fundamentals of kinematic hardening hyperplasticity, Int. J. Solids Struct. 38 (iss. 21) (2001) 3771–3794.
[10] A.M. Puzrin, G.T. Houlsby, A thermomechanical framework for constitutive models for rate-independent dissipative materials, Int. J. Plast. 16 (2001) 1017–1047.
[11] M. Ortiz, L. Stainier, The variational formulation of viscoplastic constitutive updates, Comput. Methods Appl. Mech. Eng. 171 (1999) 419–444.
[12] F. Henrotte, S. Steentjes, K. Hameyer, C. Geuzaine, Iron loss calculation in steel laminations at high frequencies, IEEE Trans. Magn. 50 (2) (2014) 333–336.
[13] P. Handgruber, A. Stermecki, O. Br, V. Gorian, E. Dlala, G. Ofner, Anisotropic generalization of vector preisach hysteresis models for nonoriented steels, IEEE Trans. Magn. 51 (3) (2015) 1–4.